Applied and Environmental Microbiology, Sept. 2010, p. 5860–5869 Vol. 76, No. 17
0099-2240/10/$12.00 doi:10.1128/AEM.00754-10
Copyright © 2010, American Society for Microbiology. All Rights Reserved.

Diffusion Measurements inside Biofilms by Image-Based Fluorescence Recovery after Photobleaching (FRAP) Analysis with a Commercial Confocal Laser Scanning Microscope▽

François Waharte,[1] Karine Steenkeste,[2] Romain Briandet,[3]* and Marie-Pierre Fontaine-Aupart[2]

Cell and Tissue Imaging Facility (PICT-IBiSA), CNRS-Institut Curie, Centre de Recherche, Paris, France[1]; Institut des Sciences Moléculaires d'Orsay, CNRS FRE 3363, Université Paris-Sud, Orsay, France[2]; and INRA, UMR 1319 MICALIS, Massy, France[3]

Received 25 March 2010/Accepted 6 July 2010

Research about the reactional and structural dynamics of biofilms at the molecular level has made great strides, owing to efficient fluorescence imaging methods in terms of spatial resolution and fast acquisition time but also to noninvasive conditions of observation consistent with *in situ* biofilm studies. In addition to conventional fluorescence intensity imaging, the fluorescence recovery after photobleaching (FRAP) module can now be routinely implemented on commercial confocal laser scanning microscopes (CLSMs). This method allows measuring of local diffusion coefficients in biofilms and could become an alternative to fluorescence correlation spectroscopy (FCS). We present here an image-based FRAP protocol to improve the accuracy of FRAP measurements inside "live" biofilms and the corresponding analysis. An original kymogram representation allows control of the absence of perturbing bacterial movement during image acquisition. FRAP data analysis takes into account molecular diffusion during the bleach phase and uses the image information to extract molecular diffusion coefficients. The fluorescence spatial intensity profile analysis used here for the first time with biofilms is supported both by our own mathematical model and by a previously published one. This approach was validated to FRAP experiments on fluorescent-dextran diffusion inside *Lactoccocus lactis* and *Stenotrophomonas maltophilia* biofilms, and the results were compared to previously published FCS measurements.

Biofilms are spatially organized populations of microorganisms associated with surfaces in any natural or man-made environment and embedded in a highly hydrated matrix made up of extracellular polymeric substances (EPS). This intercellular matrix constitutes the true interface between the cells and their environment. Convergent evidences suggest a permanent reorganization of the matrix as an adaptive response of the microbial community toward a changing environment (2, 12, 14). In response to external changes, bacteria may metabolize and/or produce a variety of organic exopolymers (polysaccharides, DNA, proteins, etc.) with different physicochemical properties. These EPS may act as a defensive barrier against aggressive environmental parameters (e.g., antimicrobials or predation by bacteriophages, protists, or phagocytes) (6, 8). A deeper understanding of the interrelations between the structure, the reactivity, and the variability of the extracellular polymeric matrix fastening together surface-associated bacteria is of major importance in the comprehension of the biofilm mode of life. For this purpose, the use of specific microelectrodes or *ex situ* analysis following extraction of polymers has been reported (7, 21). However, these approaches are invasive and poorly resolutive and do not allow dynamic observations of biofilms over time. In recent years, it has been shown that analysis of EPS properties could be greatly improved by using optical-microscopy methods that allow noninvasive *in situ* observations.

Confocal laser scanning microscopy (CLSM), in conjunction with the use of fluorescence reporters, allows direct visualization of the three-dimensional structure of spatiotemporal biofilm and its evolution under environmental stress (e.g., antimicrobials, phages, and protists). Using time lapse imaging, it is possible to track over time the mobility of free molecules in such spatially organized biosystems (16, 19). However, only average diffusion coefficients over the macrostructure are obtained, and the method is not appropriate for fast molecular diffusion. In contrast, fluorescence correlation spectroscopy (FCS) is now a well-established method of characterization of the local and fast diffusion of fluorescently labeled molecules through the depth of a biofilm (4, 10, 11). Early on, FCS was explored by means of homemade equipment by those with specialized knowledge (9, 17). Now the method can be adapted to CLSM but requires dedicated and expensive experimental setup.

To access a local resolution similar to that of FCS diffusion processes in conjunction with CLSM convenience, fluorescence recovery after photobleaching (FRAP) appears to be a good technique when the fluorophore concentration is too high for correlation measurements and sufficient for imaging. The basic principle of FRAP is to photobleach a small, spatially confined area by high-intensity laser pulses and then to observe the recovery of fluorescence inside the photobleached area as a function of time. The method has hardly ever been applied to measurements in biofilms (5, 13), and the results

* Corresponding author. Mailing address: INRA UMR 1319 MICALIS, 25 avenue de la République, 91300 Massy, France. Phone: 33 1 69 53 64 77. Fax: 33 1 69 93 51 44. E-mail: romain.briandet@jouy.inra.fr.

▽ Published ahead of print on 16 July 2010.

Downloaded from http://aem.asm.org/ on February 3, 2015 by guest

present some limitations. In the first approach (13), due to the low-frequency image acquisition of the CLSM setup, a very large biofilm area (800 μm^2) was photobleached, leading to average diffusion coefficients over the macrostructure, including water channels and clusters. In contrast, Bryers and Drummond (5) determined local diffusion coefficients in biofilm (with a photobleached surface of ~80 μm^2), using the Axelrod mathematical model (1), which precludes any molecular diffusion during the photobleaching time and is not well adapted for very common mobile molecules (e.g., fluorophores and antibacterial molecules).

We present and analyze here an image-based FRAP protocol that can be readily applied by anyone familiar with a CLSM to improve the accuracy of FRAP measurements of the molecular diffusion inside bacterial biofilms. This protocol includes (i) image acquisition of photobleached areas acquired with a commercial CLSM at high frequency, allowing bleach zones smaller than 1 μm^2; (ii) an original FRAP analysis used for the first time for measurements in biofilms that takes into account molecular diffusion during the bleach phase, which is based on fluorescence intensity profiles (18) to extract molecular diffusion coefficients; and (iii) a comparison of these results with those obtained by numerical calculation of fluorescence recovery curves, using our own analytical model and the one proposed by Braga et al. (3). This approach was validated by experiments with fluorescent-dextran diffusion inside regular *Lactoccocus lactis* biofilms and mucoid *Stenotrophomonas maltophilia* biofilms, and the results were compared to FCS data previously published. However, the proposed protocol may not lead to correct estimation of molecular diffusion coefficients if no consideration of bacterial movements is taken. Indeed, such cellular dynamics may invalidate FRAP analysis and thus indicate a need for using an appropriate visualization tool like kymogram representation. Kymograms are two-dimensional graphs of fluorescence intensity measured along a line (here a straight line drawn on the full width of the images) for each image of a time lapse acquisition. It can thus be used to show fluorescence intensity fluctuations over time along a chosen trajectory and to characterize the motion of structures present in the sample (bacteria in the present study) (15). We show for the first time that kymogram representation is a powerful tool to determine the global trends of biofilm dynamics.

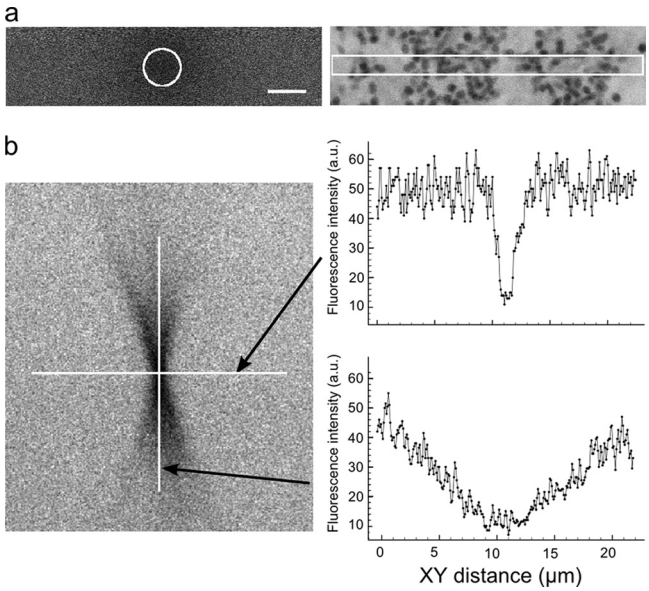

FIG. 1. Experimental conditions for image-based FRAP on biofilms, using a confocal microscope. (a) Left panel: typical image for acquisitions on FITC-dextrans in water. The white circle represents the region over which fluorescence intensity is averaged along the time series for extraction of fluorescence recovery curves. Right panel: the same conditions on a *S. maltophilia* biofilm, showing the importance of spatial information gained by the use of images. The white rectangle shows the size of the image used in Braga et al. (3), too small to be useful for biofilm experiments. (b) Left panel: *xz* image of the photobleaching pattern on fluorescent plastic. Intensity profiles in *xy* (upper right panel) and in *z* (lower right panel) were measured along the crossed lines. The scale bar represents 5 μm. a.u., arbitrary units.

MATERIALS AND METHODS

Biofilm growth. Two bacterial strains were used: *Stenotrophomonas maltophilia* 114N-Sm, a Gram-negative spoilage bacterium isolated on a surface in a dairy plant, and the Gram-positive dairy starter *Lactoccocus lactis* subsp. *cremoris* 14N-Ll (10). Stock cultures were prepared by mixing stationary-growth-phase cultures with a 40% (vol/vol) glycerol solution. *S. maltophilia* 114N-Sm was cultivated in trypticase soy broth ([TSB] bioMérieux, France), and *L. lactis* strains were cultivated in M17 broth (BD-Difco, France) supplemented with 0.5% glucose. All bacteria were grown at 30°C, and two subcultures were realized before a last overnight culture. Bacterial cultures were harvested by centrifugation (7,000 × *g*; 4°C; 10 min.) and washed twice in NaCl 150 mM. The bacterial concentration was fitted to 10^8 CFU/ml by adjusting absorbance at 400 nm. Biofilm formation was performed on a glass surface of 4-well sterile microscopic chambers (Lab-Tek; Nalge Nunc, Naperville, IL). Two milliliters of the suspension was poured into each sterile well of the chambers and incubated for 1 h at 30°C to allow initial attachment. Planktonic nonadherent cells were then washed out by refilling the wells three times with NaCl 150 mM. Contaminated wells were then filled with 2 ml of growth media and incubated at 30°C for 24 h to allow biofilm development.

FRAP measurements of FITC-dextrans in biofilms. Dextrans (polymers of anhydroglucose) labeled with fluorescein isothiocyanate (FITC) were used as follows in the experiments (FITC is conjugated randomly to hydroxyl groups of dextrans at a frequency of 0.003 to 0.020 mol of FITC per mole of glucose). One hundred fifty kilodaltons of FITC-dextrans (Sigma Aldrich, Saint-Quentin Fallavier, France) were dissolved to 15 mg/ml in water, which corresponds to a concentration of 10^{-4} mol · liter^{-1}. For FRAP experiments, 100 μl of this solution was then added to previously rinsed biofilms. They were then imaged on an inverted Leica TCS SP5 confocal microscope (Leica Microsystems, Wetzlar, Germany) with an oil-immersion 63× objective of numerical aperture (NA) of 1.4. FITC-dextran fluorescence was excited with the 488-nm laser line of an argon laser and detected on a 500- to 650-nm spectral bandwidth. All experiments were performed at ~20°C.

The conditions of FRAP experiments were optimized, using 150 kDa of free FITC-dextran in water. Fluorescence intensity image size was fixed to 512 by 128 pixels with an 80-nm pixel size to ensure usable spatial information on the biofilm (~40 × 10 μm^2) (Fig. 1a). For a 1,400-Hz line scan rate, the total time between frames was ~205 ms. Fluorescence intensity images were recorded, using 16-bit resolution to improve image analysis.

For imaging the three-dimensional bleached volume, a green fluorescent plastic slide sample was bleached for 5 s at the maximum laser intensity; a *z*-stack of 326 images was then acquired in the bleached area, with a distance between each image of 0.1 μm. The two-dimensional image size was 128 by 128 pixels, with a pixel size of 114 nm. The full widths at half maximum (FWHM) in *xy* and *z* (along the optical axis) of the bleached profile were then estimated at 0.8 μm and 14 μm, respectively (Fig. 1b).

Each FRAP experiment started with the acquisition of 50 image scans acquired at 10% of the maximum laser intensity (which was measured to be ~350 μW at the object level), followed by a bleach pulse of 50 ms at 100% laser intensity on a 0.8-μm-diameter spot. A series of 300 single-section images were then collected at 205-ms intervals, the first image being acquired 630 ms after the beginning of bleaching. For imaging after photobleaching, the laser power was

Downloaded from http://aem.asm.org/ on February 3, 2015 by guest

attenuated to its initial value (10% of the bleach intensity). Under these image acquisition conditions, FRAP measurements could be acquired in 70 s, and bacterial viability was controlled with live-dead stain labeling.

It must be noted that the goal is to reach the best compromise between two-dimensional image size and time resolution. In consequence, image acquisition frame rates are constrained. Increasing acquisition frame rates would require reducing the region size and therefore precludes the acquisition of large biofilm sections, as illustrated in Fig. 1a.

FRAP analysis. In order to define a well-adapted theoretical model for FRAP analysis, we first investigated the influence of the presence of bacteria on fluorophore diffusion (a nonhomogenous medium) by Monte Carlo simulations (data not shown). Simulated fluorescence recovery curves were similar in the absence and in the presence of obstacles corresponding to the bacteria. Thus, as for most previously reported data (5, 13), in this study we considered pure isotropic diffusion in a homogenous medium.

Furthermore, considering the ratio between the axial (14 μm) and the lateral (0.8 μm) extent of the photobleaching pattern, diffusion along the axial/vertical axis can be neglected; thus, only two-dimensional diffusion was considered.

Fluorescence recovery curves were extracted, using the circular region of 25 μm^2 inside the photobleached region, as shown in Fig. 1a.

Intensity profile analysis method. During the photobleaching phase, diffusion occurred and led to the widening of the photobleached region (see Fig. 4). The profile width of this zone was extracted by fitting a series of intensity profiles obtained from images taken during the recovery process with a Gaussian function:

$$I(x) = I_0 e^{-\frac{2(x - x_0)}{d^2}} + K$$

where K is a constant and x_0 is the center of the profile. The width d is related to the diffusion coefficient by the formula $d^2 = 8Dt$ for a two-dimensional diffusion process. Therewith it is possible to determine the diffusion coefficient by plotting d^2 as a function of time and using linear regression to estimate the slope of the graph, keeping only the first 6 to 10 images (corresponding to the first 2 s of recovery). This procedure was implemented with the macro language included in ImageJ software version 1.43 (http://rsbweb.nih.gov/ij/) and is available upon request (Francois.Waharte@curie.fr).

The speed-optimized image acquisition conditions gave noisy images. To reduce noise, we measured an azimuthally averaged line profile centered on the photobleached region of the few first images of the series (typically 20 images) after the photobleaching phase. This process consists of measuring intensity profiles along a rotating line centered on the photobleached area and calculating the mean of each pixel of the line for all angles. For the data presented here, we used a 30° rotation with a 180-pixel line length (on images of 512 by 128 pixels).

This intensity profile analysis method was validated by using synthetic data generated by calculation of an analytical solution of a two-dimensional diffusion equation, as described below (equation 5; see Fig. 4a and b). A large range of diffusion coefficients named D_{th} was applied. Using the procedure described above, we extracted the square of the intensity profile width and showed that it varied linearly with time (see Fig. 4c). Furthermore, we also verified that the diffusion coefficient thus estimated [slope of the curve, $d^2 = f(t)$; see Fig. 4c] corresponds to the D_{th} values.

Analytical models and data fitting. Postbleach fluorescence recovery in FRAP experiments using an analytical solution of the diffusion equation was simulated for both the validation of intensity profile analysis (see above) and the fitting of fluorescence recovery curves.

Considering free and isotropic diffusion on an infinite xy plane, the evolution of the unbleached fluorophore concentration (C) follows the classical diffusion equation:

$$\frac{\partial C}{\partial t}(x,y,t) = D\Delta C(x,y,t) \quad (1)$$

This diffusion equation can be solved by convolution of the initial concentration, $C_o(x,y)$, with the Green function, $G(x,y,t)$:

$$C(x,y,t) = C_0(x,y) \cdot G(x,y,t), \quad (2)$$

Considering a Gaussian intensity profile of the laser, $C_o(x,y)$ is defined as:

$$C_0(x,y) = C_0 e^{-\frac{2(x^2 + y^2)}{\omega^2}}, \quad (3)$$

and $G(x,y,t)$ by:

$$G(x,y,t) = \frac{1}{4\pi Dt} e^{-\frac{x^2 + y^2}{4Dt}}, \quad (4)$$

D being the diffusion coefficient and ω the laser width.

According to equations 3 and 4, the diffusion equation can be written as follows:

$$C(x,y,t) = \frac{C_0\omega^2}{8Dt + \omega^2} e^{-\frac{2(x^2 + y^2)}{8Dt + \omega^2}} \quad (5)$$

We implemented the calculation of FRAP recovery image sequences by using expression (5) in a custom-written C++ software based on the CImg image manipulation library (http://cimg.sourceforge.net/).

Fluorescence recovery curves were extracted from the simulated data by measuring the mean fluorescence intensity in the region defined in Fig. 1a, using ImageJ software. Data fitting using our model was obtained by manually comparing these theoretical curves to experimental data after normalization of both curves between 0 (start of recovery) and 1 (end of recovery), using plotting software (Plot 0.997; http://plot.micw.eu/).

Data were also analyzed according to the model from Braga et al. (3). Equation 9 from Braga et al. was implemented in Excel spreadsheet software (Microsoft, Inc.), keeping only the first three terms of the series in the expression. Data fitting was done using the Excel solver tool.

RESULTS

Acquisition of FRAP time series images with a confocal microscope. Some typical FRAP experiments with FITC-dextrans in both *L. lactis* and *S. maltophilia* biofilms are presented in Fig. 2a and d, respectively. Images of the biofilms were taken before and after bleaching, with a 205-ms time interval between images. On these images, unlabeled bacterial cells were visible in dark gray, and the photobleached area at the centers of the images appeared darker. These images later disappeared progressively in-line with the diffusion of FITC-dextrans in the biofilms. The quantification of fluorescence recovery in the photobleached area can be visualized over time as presented in Fig. 2b and e. In these graphs, the fluorescence stabilization in the photobleached areas reached a value at least 95% of the initial value after ~30 s. A control experiment was performed, using the same experimental conditions but without the photobleaching phase; a very slight decrease in fluorescence was observed during the acquisition time (the final value was >95% of the initial value) due to probe photobleaching. As nearly complete fluorescence recovery of all the FITC-dextrans was observed (>95% of the initial fluorescence), we assume that the immobile fraction of FITC-dextrans is negligible (there was no measurable interaction of dextrans with bacterial cell walls in our conditions) and that all the molecules were diffusing.

Even if these fluorescence recovery curves appear to have a correct shape (Fig. 2b and e), they are not sufficient to check biofilm stability during the measurements. We thus show the corresponding kymograms in Fig. 2c and f. When bacteria do not move, this representation leads to continuous adjacent vertical lines, as observed in both fields presented in Fig. 2c and f. When a motion of the biomass occurs during FRAP acquisitions, the corresponding kymograms are distorted (Fig. 3c, f, and i). This movement can induce fluctuations of the fluorescence intensity in the bleached region, impairing quantitative analysis (Fig. 3b, e, and h).

Different cases may be observed. (i) Lateral global movement of the biofilm cells as revealed by the distorted kymogram presented in Fig. 3g. In this kymogram, lines are clearly

Downloaded from http://aem.asm.org/ on February 3, 2015 by guest

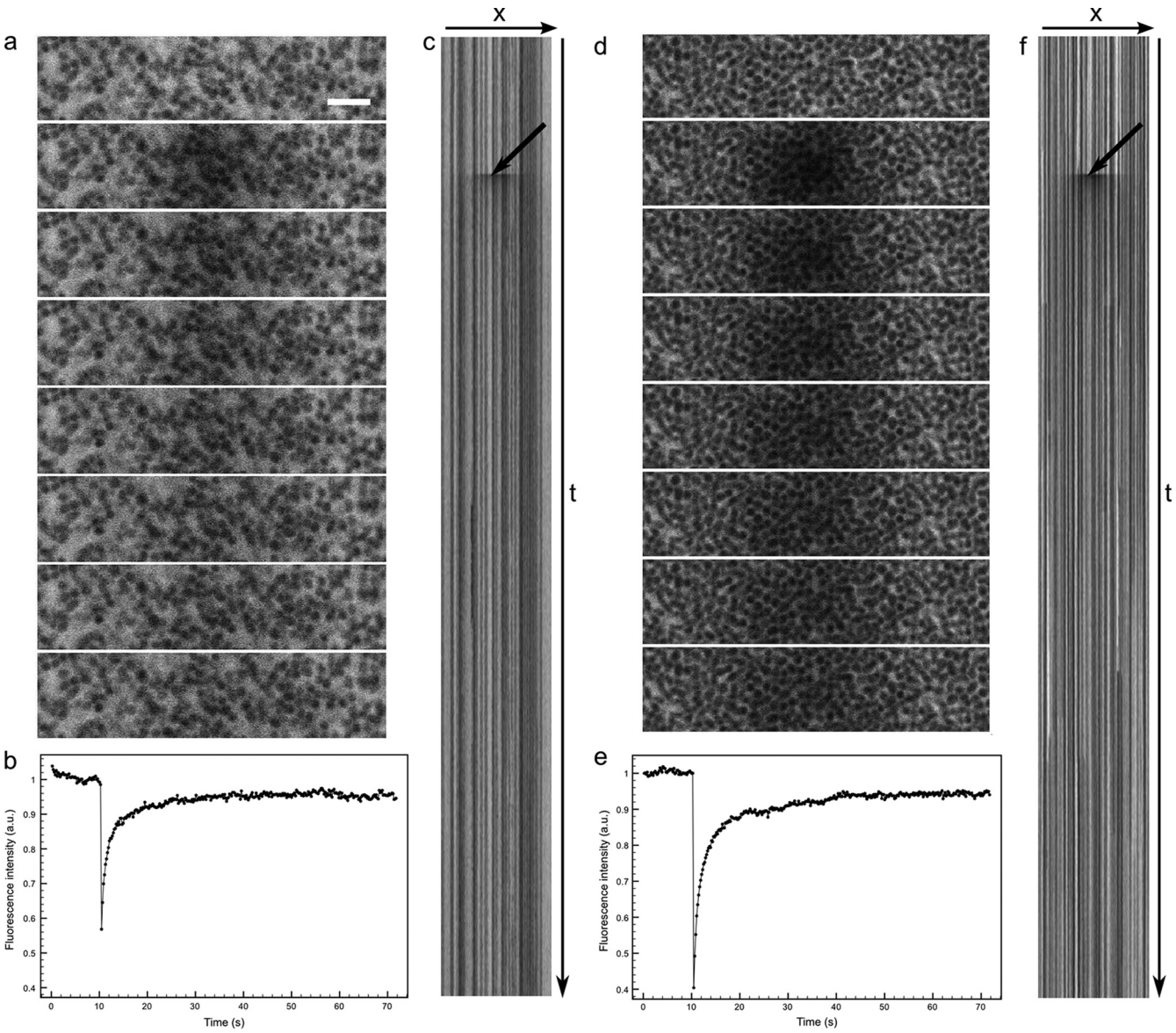

FIG. 2. Examples of correct FRAP acquisitions on both types of biofilms. (a and d) Image sequence starting just before photobleaching and showing the beginning of the recovery phase for *L. lactis* (a) and *S. maltophilia* (d). (b and e) Corresponding fluorescence recovery curve (over the full sequence) for *L. lactis* (b) and *S. maltophilia* (e). (c and f) Kymogram representation (xt) of the same sequence (black arrows indicate the start of the recovery) for *L. lactis* (c) and *S. maltophilia* (f). The time interval between two images is 205 ms. The scale bar represents 5 μm.

deviated from verticality after photobleaching; apparently satisfactory fluorescence recovery curves (Fig. 3h) are observed with almost total fluorescence recovery, but the diffusion coefficient can be significantly altered. Using the Braga model, we obtained from this curve a coefficient diffusion (D) value of $\sim$1 $\mu m^2 \cdot s^{-1}$, compared to $\sim$8 $\mu m^2 \cdot s^{-1}$ (see latter) in the absence of biomass movements.

(ii) Appearance or detachment of cells or clusters during acquisition due to immigration from or emigration to neighboring fields, as presented in Fig. 3d and Fig. 3a, respectively. In this case, both kymograms (Fig. 3c and f) and fluorescence recovery curves (Fig. 3b and e) are strongly altered. Kymograms are not continuous; new lines appear or disappear during the time series after photobleaching. The chaotic structures of these fluorescence intensity curves stress out the sample disturbance during the acquisition.

Visualization of kymograms from raw FRAP time series data appears to be a more powerful tool than the conventional fluorescence recovery curves. Furthermore, it is in some cases essential in order to discard distorted acquisitions (Fig. 3 h). Once the quality of the data are validated by such pretreatments, the series can be used to calculate the local diffusion coefficients. Different methods were used and compared to the published Braga model for intracellular macromolecular mobility (3).

Determination of the local diffusion coefficient by intensity profile analysis. The first method implemented relies on analysis of photobleached-region spreading by the measurement of

Downloaded from http://aem.asm.org/ on February 3, 2015 by guest

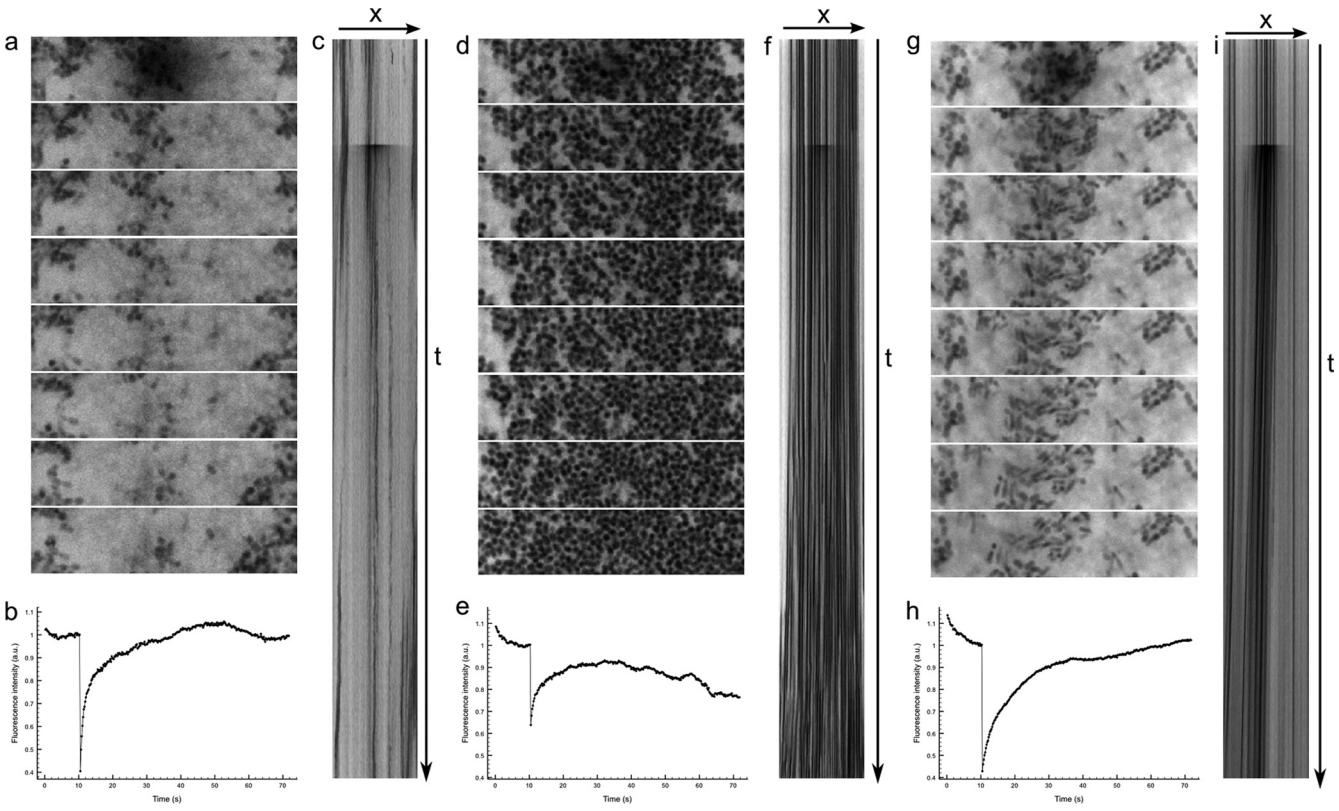

FIG. 3. Image sequences during FRAP experiments, showing potential difficulties for data exploitation. (a through c) Sequence with global drift of the biofilm. (d through f) Influence of bacterial motion on FRAP sequence. (g through i) Photo-induced contraction of biofilm The image size is about 40 by 10 μm^2.

fluorescence intensity profiles. The method developed by Seiffert and Oppermann (18) allows consideration of only the postbleaching phase of FRAP experiments and takes into account the spreading of the photobleached area due to diffusion during the bleaching phase.

We first validated this approach and our analysis tools on calculated image sequences (Fig. 4a, b, and c), as explained in the Materials and Methods section. We then applied the intensity profile analysis method on fluorescent dextrans (150 kDa) in aqueous solution (Fig. 4d, e, and f) and estimated a diffusion coefficient of $\sim$14 $\mu m^2 \cdot s^{-1}$ from the line slope derived from the representation of the square of the intensity profile width as a function of time. This value was underestimated in comparison to the theoretical prediction from the Stokes Einstein equation ($D = 24\ \mu m^2 \cdot s^{-1}$ at 20°C with a hydrodynamic radius of 150 kDa of FITC-dextrans; $R = 8.5$ nm) with respect to a relatively low frequency of image acquisition, as discussed below.

This analysis was extended to FITC-dextrans inside *L. lactis* and *S. maltophilia* biofilms (Fig. 5). With kymogram representation showing no biomass movement during FRAP experiments (data not shown), it was possible to almost eliminate the spatial heterogeneities in the fluorescence images due to the presence of bacteria (Fig. 5a and c). For this purpose, we divided all postbleach images by the mean prebleach images and then applied a smoothing filter on the resulting image stack (Fig. 5b and d). The image stack obtained after this treatment shows more clearly the photobleached area than the original image stack. The intensity profiles extracted from this treated image sequence are smoothed, are far less noisy, and hence are better fitted by a Gaussian function (compare profiles in Fig. 5a and c with those in Fig. 5b and d).

In all cases, we observed a linear variation of the squared width of the intensity profile over time, as observed with free FITC-dextrans (Fig. 4f), that validated the assumption of a pure diffusion process despite the presence of bacteria.

The diffusion coefficient values of different experimental data sets from both types of biofilms were estimated, and the dispersion result is given in Fig. 5e. From all these experiments, we obtained mean diffusion coefficient values of 10 ± 5 $\mu m^2 \cdot s^{-1}$ and 20 ± 4 $\mu m^2 \cdot s^{-1}$ for FITC-dextrans in *S. maltophilia* and *L. lactis*, respectively, revealing mobility impairment in *S. maltophilia* biofilms.

Determination of the local diffusion coefficient by mathematical modeling. We also used mathematical models to perform quantitative analysis of FRAP measurements. First, we extracted the fluorescence recovery curves from image sequences for both types of biofilms and normalized all curves to 1 for the prebleach intensity (Fig. 6). This allowed direct comparison of every curve and checks for artifacts. For example, curves with a marked decrease in intensity at the end of the recovery indicate significant photobleaching of the sample (Fig. 6c, arrowed curve). On others, irregular curves with sometimes higher intensity than the initial values likely reflect

Downloaded from http://aem.asm.org/ on February 3, 2015 by guest

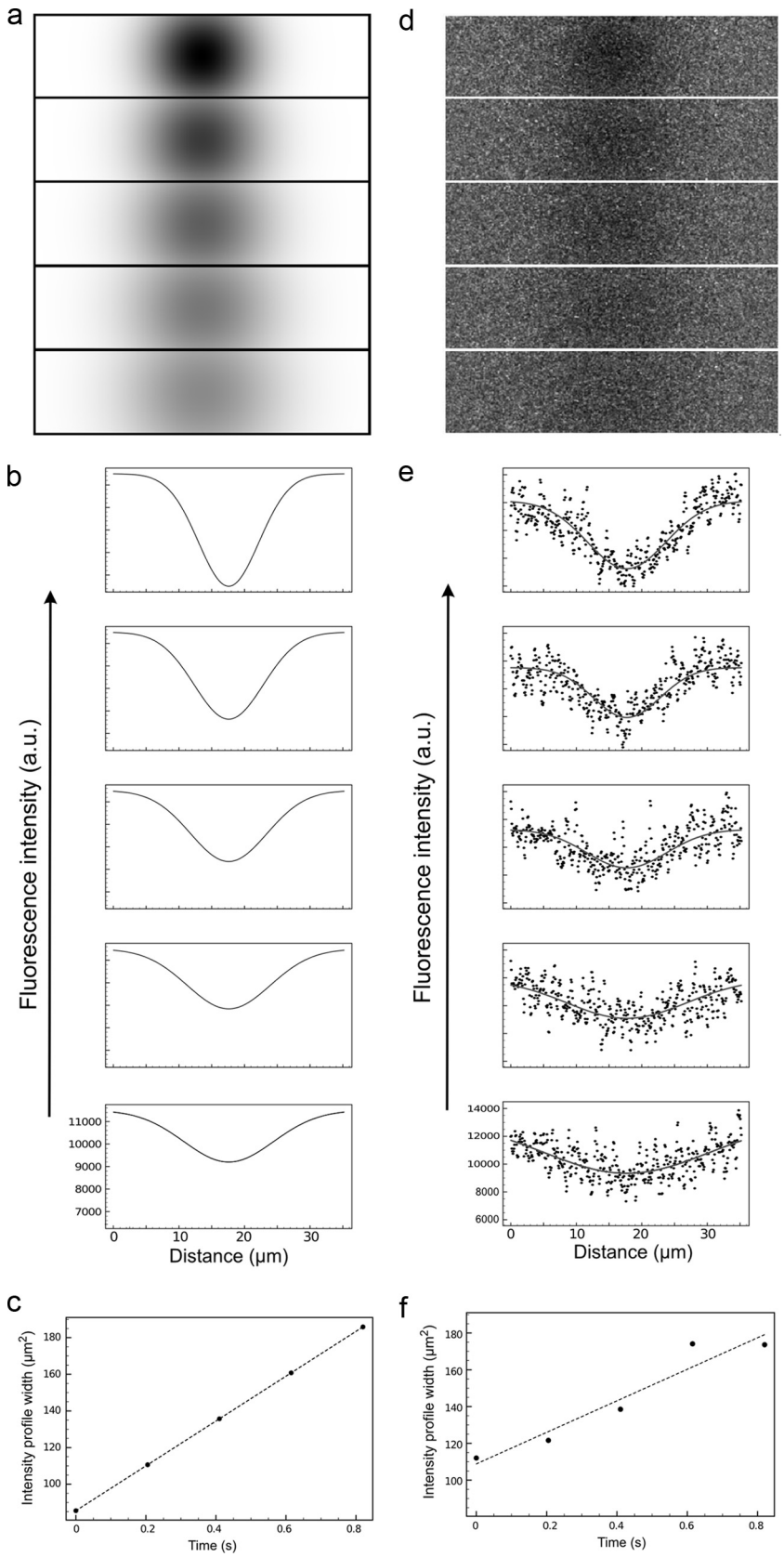

FIG. 4. Determination of the diffusion coefficients by image analysis using the intensity profile method. (a) Image sequence after photobleaching, showing the beginning of recovery for calculated images from equation 2. (d) Image sequence of FITC-dextrans in water. (b) Successive intensity profiles across the photobleached region. (e) Successive intensity profiles of FITC-dextrans in water. (c) Graph of the squared profile width as a function of time. (f) Graph of the squared profile width of FITC-dextrans in water. The time interval between two images is 205 ms. The image size is about 40 by 10 μm^2.

Downloaded from http://aem.asm.org/ on February 3, 2015 by guest

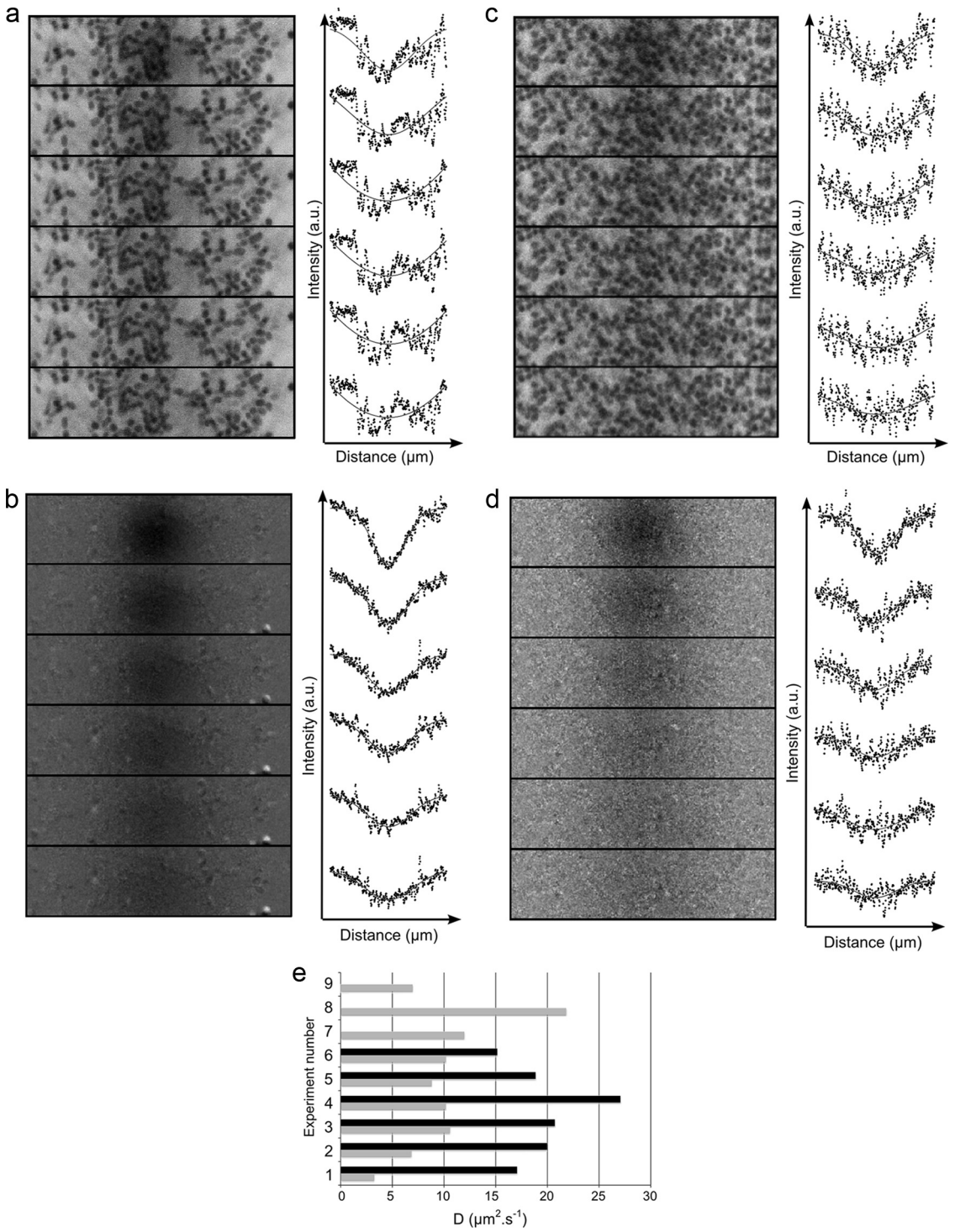

FIG. 5. Application of the intensity profile method to biofilm data. (a and c) Left panel: raw image sequence after photobleaching on *S. maltophilia* (a) and *L. lactis* (c) biofilms. Right panel: corresponding intensity profiles with Gaussian fit used to extract the profile width. (b and d) Same sequence and intensity profiles after image treatment to reduce heterogeneity on *S. maltophilia* (b) and *L. lactis* (d) biofilms. (e) Representation of dispersion of estimated diffusion coefficients for both types of biofilms. Results for *L. lactis* are shown in black and for *S. maltophilia* in gray. The time interval between two images is 205 ms. The image size is about 40 by 10 μm^2.

laser fluctuations (Fig. 6b, arrowed curve). In both cases, the curves were rejected.

As a first application, our own calculations (see Materials and Methods, equation 5) and the two-dimensional model of Braga et al. (3) were used to determine the diffusion coefficients of 150 kDa of FITC-dextrans in aqueous solution. Both methods always gave very close D values of 10 to 11 $\mu m^2 \cdot s^{-1}$, similar to those obtained with intensity profile analysis (Fig. 6a).

Downloaded from http://aem.asm.org/ on February 3, 2015 by guest

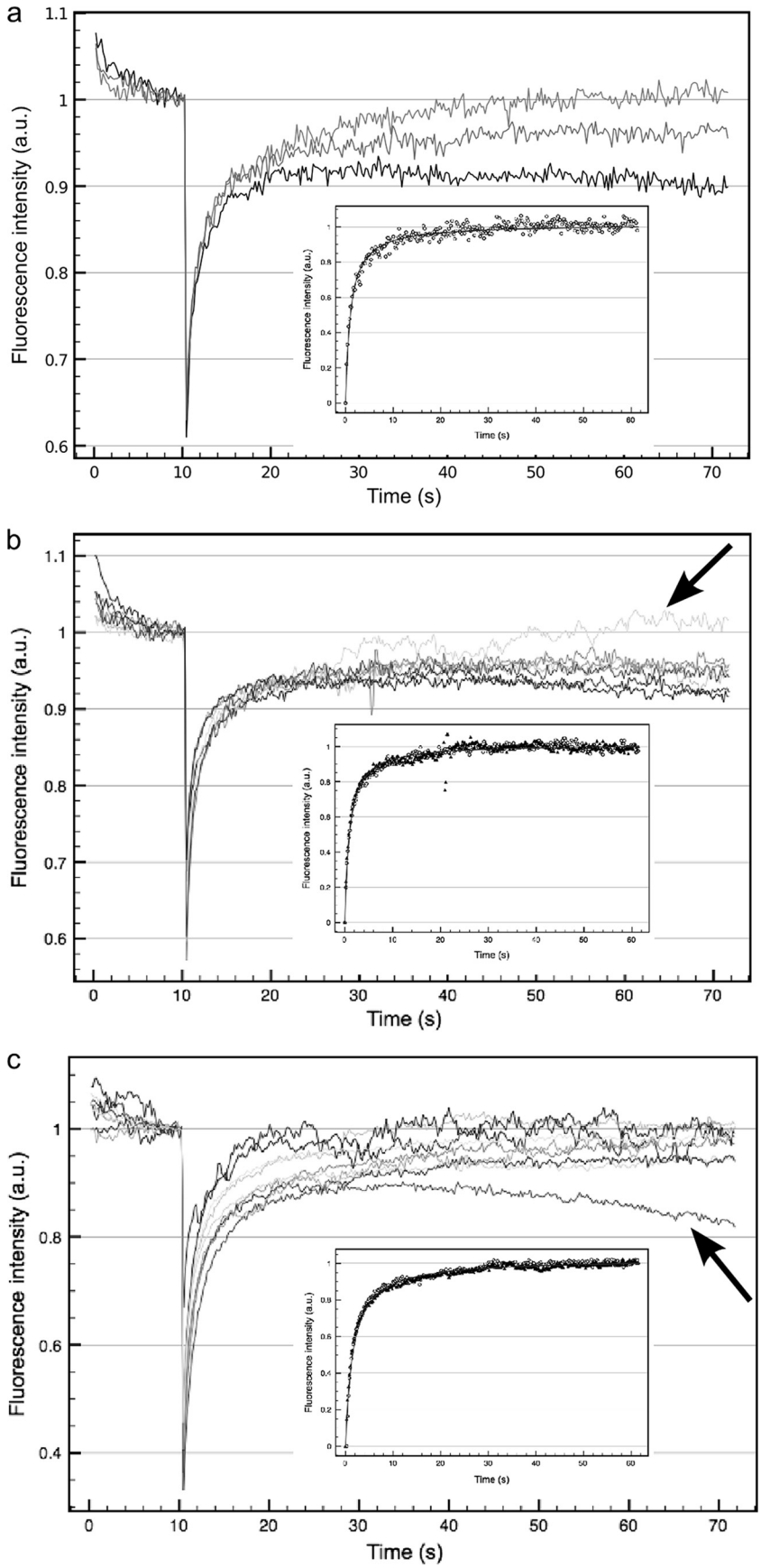

FIG. 6. Diffusion coefficient estimation by analytical models. Summary of fluorescence recovery curves for FITC-dextrans in water (a), FITC-dextrans in *L. lactis* biofilms (b), and FITC-dextrans in *S. maltophilia* biofilms (c). Selected curves were adjusted, using our model (inset). Arrows in panels b and c indicate fluorescence recovery curves that were rejected, as explained in Results.

Downloaded from http://aem.asm.org/ on February 3, 2015 by guest

Normalized FITC-dextran fluorescence recovery curves in *L. lactis* biofilms are poorly dispersed (Fig. 6b). Their fitting gave diffusion coefficient values rather similar to those in pure water, with D values of 10 to 13 $\mu m^2 \cdot s^{-1}$ (Fig. 6b, inset), regardless of the analytical expression used (our model or the Braga model).

There was greater variability between the different FITC-dextran fluorescence recovery curves of *S. maltophilia* biofilms (Fig. 6c) than between those of the *L. lactis* biofilms. This variability was likely due to the structural heterogeneity of the biofilm and/or variations in the local concentration of fluorophores that leads to different photobleaching amplitudes between 50 and 70% (compared to 30 to 40% for *L. lactis*). Nevertheless, from selected curves (showing monotonous variation with maximal values below the initial fluorescence intensity and sufficient signal quality) we could estimate a diffusion coefficient value, D, of 7 to 8 $\mu m^2 \cdot s^{-1}$ with both models.

DISCUSSION

The improvement in quality of commercial CLSMs in terms of sensitivity and image acquisition rate and the development of dedicated analysis methods allow increases in the performance of FRAP experiments and have renewed interest in the method to characterize molecular mobility in various biological systems.

A classical FRAP experiment is followed only on a time scale and viewed as fluorescence recovery curves. But using CLSM, FRAP can also be analyzed on a spatial scale, exploiting information included in image-time series, which implies reaching a compromise between the spatial extent of images and the temporal resolution of data acquisition. In our case, we worked on image sequences of 512 by 128 pixels, with a 205-ms time interval, which gave already satisfactory information on the biofilm structure and dynamics essential for validation of diffusion process quantification. Indeed, inside biofilms, intrinsic or artifactual bacterial motion (individual active or passive motion or global drift) can occur. We demonstrated that the application of a kymogram representation gives access to such bacterial motion and allows elimination of some fluorescence recovery curves that correspond to unworkable acquisitions (Fig. 3a and g). These motions were not taken into account in previous FRAP studies of biofilms, due to a lower image acquisition rate or lack of image analysis tools (5, 13).

Interest in performing FRAP experiments based on image sequences is also due to the ability to extract information on molecular diffusion directly from the evolution of the temporal-intensity profile. Then the evaluation of diffusion coefficients in biofilms, based only on experimental support without any calibration measurements, is easy and straightforward. Furthermore, in comparison to analytical models, this approach does not require a strong mathematical background and can be readily implemented on any workstation, using, for example, ImageJ software and the dedicated macro program that we developed and provided to the community. The reliability of this image-based method was supported by comparison of the coefficient diffusion values thus determined with those obtained with our analytical model and with the one proposed by Braga et al. (3). Indeed, regardless of which model was used, the values were of the same order of magnitude and showed the same trend: diffusion is always slower in *S. maltophilia* biofilms than in water or in *L. lactis* biofilms.

Analyzing the fluorescence intensity profile by the method presented here also provides the possibility of obtaining, as a complement to the kymogram representations, information on the spatial evolution of the photobleached region. Indeed, any fluorophore convection (flow) would lead to a displacement of the profile center and fluorophore diffusion anisotropy to a change in profile symmetry, which was not observed in these biofilm measurements (Fig. 5). In other biological systems, such intensity profile distortions could be quantified to obtain information on local heterogeneity that would require a dedicated analytical model.

Nevertheless, this approach to FRAP measurement analysis presents some limitations, one being its sensitivity to the signal-to-noise ratio of the images. This can be less apparent when analyzing fluorescence recovery curves extracted by averaging the intensity over a whole area (tens of pixels in this study). Another limitation is the necessity of making a compromise between the image acquisition rate and the image size to retain spatial information on the biofilm structure. In respect to these conditions, in the present experiments, the time interval between frames was fixed to 205 ms; thus, fluorescence recovery was observable only on the first five images (Fig. 4). Moreover, due to constraints of the microscope, there was a long delay (630 ms) between the last prebleached and the first postbleached images, leading to loss of the beginning of the fluorescence recovery. Thus, for such image sequencing, the time of origin of the analysis is significantly delayed relative to the end of bleaching, leading to underestimated diffusion coefficients. This is also true of FRAP data analysis using mathematical models. For example, we obtained a value of ~10 to 14 $\mu m^2 \cdot s^{-1}$ for 150 kDa of FITC-dextrans in water (depending on the analysis method), which must be compared to the theoretical and previous FCS values (10) of 24 $\mu m^2 \cdot s^{-1}$. This problem could be countered by using a different CLSM instrument with better performance for image acquisition or, in our case, by reducing the image size, leading to an increase in image acquisition frequency. However, even if diffusion coefficients are underestimated, qualitative comparison of the values in different environments can be done successfully.

In addition to the intensity profile method, the fluorescence recovery curves were fitted by using a simple analytical expression for spatiotemporal fluorophore concentration evolution that considers a Gaussian postbleach profile. This approach has a major advantage over classical models (1) in that it takes into account diffusion during the photobleaching phase, which often occurs under the usual experimental conditions (3, 20). It must be noted that even for an arbitrary profile shape, the convolution approach by the Green function can be used (equation 2), but in this case, an analytical solution cannot be obtained; only a numerical solution can.

As a biological application, the image-based FRAP protocol and its corresponding analysis described in this paper were used to compare the diffusion rates of 150 kDa of FITC-dextrans inside *L. lactis* and *S. maltophilia* biofilms. The results can be directly compared to previous ones obtained by FCS (4, 10, 11) and help to provide an answer to the question, Does FRAP give the same information as FCS? Both methods revealed that the probe diffusion coefficient value was lower and

Downloaded from http://aem.asm.org/ on February 3, 2015 by guest

more dispersed for *S. maltophilia* biofilms than for *L. lactis* biofilms (D = ~10 $\mu m^2 \cdot s^{-1}$ and 20 $\mu m^2 \cdot s^{-1}$, respectively). As mentioned previously (10), this difference in FITC-dextran behavior between the two biofilms is in accordance with their dissimilarity in spatial architecture. *S. maltophilia* biofilms consist of a basal layer of cells decorated with heterogeneous, three-dimensional, compact aggregates rich in EPS that could be compared to the "mushroom-like" structure frequently described for other Gram-negative strains. In contrast, *L. lactis* biofilms are a regular assembly of cells embedded in a highly hydrated uniform matrix. With respect to these results, FRAP appears to be a more accessible, easier, and more attractive method than FCS to study such *in situ* diffusion processes. Furthermore, contrary to common belief, FRAP was not destructive to the biological molecules under our experimental conditions. We have also validated that FRAP allows collection of images of the sample with all the benefits already discussed. Another important feature concerns the difficulty sometimes encountered in acquiring FCS measurements due to the necessity of using very low concentrations (leading to a low level of fluorescence signals and thus a low level of performance of the fluorescence detection system), a problem which can be avoided with the FRAP method. However, in this high-concentration regimen, the sensitivity to processes other than pure diffusion is reduced because only the average behavior of a set of molecules is observed. For example, since the single-molecule level can be reached with FCS, we have observed and pointed out cases in which no correlation signal was recorded in *S. maltophilia* biofilms due to the interaction of FITC-dextrans with a component of the EPS matrix (10), whereas with FRAP, we always observed a fluorescence recovery signal. However, this signal deviated from ideal behavior in an aqueous environment (D = ~10 to 11 $\mu m^2 \cdot s^{-1}$ in water and D = ~7 to 8 $\mu m^2 \cdot s^{-1}$ in the biofilm, as determined by the mathematical models), even in the context of a simple diffusion model. Molecular interactions with the biofilm components could be better characterized and quantified with an extended model (reaction-diffusion) for FRAP analysis. This would be of great interest, in particular for highly reactive compounds such as antimicrobial agents; the use of a model containing both diffusion and reaction processes could help distinguish two agents with the same diffusivity but different antimicrobial activities.

In conclusion, we described an experimental protocol (image acquisition, data sorting, and dedicated analysis tools) based on the analysis of image sequences after fluorescence photobleaching (FRAP), which is accessible using any commercial CLSM. This protocol allows study of molecular diffusion inside biofilms in a nondestructive manner.

The spreading of a method that is so simple to set up and that gives biologically relevant information should facilitate the analysis of dynamic processes inside such spatially structured biological systems and be used as an initial and/or complementary method to FCS.

ACKNOWLEDGMENTS

We acknowledge the PRISME network of Optics Valley and the University of Orsay for funding of the confocal microscope. This work benefits from the support of Sanofi Aventis.

REFERENCES

1. **Axelrod, D., D. E. Koppel, J. Schlessinger, E. Elson, and W. W. Webb.** 1976. Mobility measurement by analysis of fluorescence photobleaching recovery kinetics. Biophys. J. **16:**1055–1069.
2. **Barken, K. B., S. J. Pamp, L. Yang, M. Gjermansen, J. J. Bertrand, M. Klausen, M. Givskov, C. B. Whitchurch, J. N. Engel, and T. Tolker-Nielsen.** 2008. Roles of type IV pili, flagellum-mediated motility and extracellular DNA in the formation of mature multicellular structures in *Pseudomonas aeruginosa* biofilms. Environ. Microbiol. **10:**2331–2343.
3. **Braga, J., J. M. P. Desterro, and M. Carmo-Fonseca.** 2004. Intracellular macromolecular mobility measured by fluorescence recovery after photobleaching with confocal laser scanning microscopes. Mol. Biol. Cell **15:**4749–4760.
4. **Briandet, R., P. Lacroix-Gueu, M. Renault, S. Lecart, T. Meylheuc, E. Bidnenko, K. Steenkeste, M. N. Bellon-Fontaine, and M. P. Fontaine-Aupart.** 2008. Fluorescence correlation spectroscopy to study diffusion and reaction of bacteriophages inside biofilms. Appl. Environ. Microbiol. **74:**2135–2143.
5. **Bryers, J. D., and F. Drummond.** 1998. Local macromolecule diffusion coefficients in structurally non-uniform bacterial biofilms using fluorescence recovery after photobleaching (FRAP). Biotechnol. Bioeng. **60:**462–473.
6. **Costerton, J. W.** 2007. The biofilm primer, 1st ed., vol. 1, p. 56. Springer-Verlag, Berlin, Germany.
7. **Cronenberg, C. C. H., and J. C. van den Heuvel.** 1991. Determination of glucose diffusion coefficients in biofilms with micro-electrodes. Biosens. Bioelectron. **6:**255–262.
8. **Flemming, H.-C., T. R. Neu, and D. J. Wozniak.** 2007. The EPS matrix: the "house of biofilm cells." J. Bacteriol. **189:**7945–7947.
9. **Guiot, E., M. Enescu, B. Arrio, G. Johannin, G. Roger, S. Tosti, F. Tfibel, F. Mérola, A. Brun, P. Georges, and M. P. Fontaine-Aupart.** 2000. Molecular dynamics of biological probes by fluorescence correlation microscopy with two-photon excitation. J. Fluoresc. **10:**413–419.
10. **Guiot, E., P. Georges, A. Brun, M. P. Fontaine-Aupart, M. N. Bellon-Fontaine, and R. Briandet.** 2002. Heterogeneity of diffusion inside microbial biofilms determined by fluorescence correlation spectroscopy under two-photon excitation. Photochem. Photobiol. **75:**570–578.
11. **Lacroix-Gueu, P., R. Briandet, S. Lévêque-Fort, M.-N. Bellon-Fontaine, and M.-P. Fontaine-Aupart.** 2005. In situ measurements of viral particles diffusion inside mucoid biofilms. C. R. Biol. **328:**1065–1072.
12. **Lawrence, J. R., G. D. W. Swerhone, U. Kuhlicke, and T. R. Neu.** 2007. In situ evidence for microdomains in the polymer matrix of bacterial microcolonies. Can. J. Microbiol. **53:**450–458.
13. **Lawrence, J. R., G. M. Wolfaardt, and D. R. Korber.** 1994. Determination of diffusion coefficients in biofilms by confocal laser microscopy. Appl. Environ. Microbiol. **60:**1166–1173.
14. **Ma, L., M. Conover, H. Lu, M. R. Parsek, K. Bayles, and D. J. Wozniak.** 2009. Assembly and development of the *Pseudomonas aeruginosa* biofilm matrix. PLoS Pathog. **5:**e1000354.
15. **Racine, V., M. Sachse, J. Salamero, V. Fraisier, A. Trubuil, and J.-B. Sibarita.** 2007. Visualization and quantification of vesicle trafficking on a three-dimensional cytoskeleton network in living cells. J. Microsc. **225:**214–228.
16. **Rani, S. A., B. Pitts, and P. S. Stewart.** 2005. Rapid diffusion of fluorescent tracers into Staphylococcus epidermidis biofilms visualized by time lapse microscopy. Antimicrob. Agents Chemother. **49:**728–732.
17. **Schwille, P., J. Bieschke, and F. Oehlenschläger.** 1997. Kinetic investigations by fluorescence correlation spectroscopy: the analytical and diagnostic potential of diffusion studies. Biophys. Chem. **66:**211–228.
18. **Seiffert, S., and W. Oppermann.** 2005. Systematic evaluation of FRAP experiments performed in a confocal laser scanning microscope. J. Microsc. **220:**20–30.
19. **Takenaka, S., B. Pitts, H. M. Trivedi, and P. S. Stewart.** 2009. Diffusion of macromolecules in model oral biofilms. Appl. Environ. Microbiol. **75:**1750–1753.
20. **Waharte, F., C. M. Brown, S. Coscoy, E. Coudrier, and F. Amblard.** 2005. A two-photon FRAP analysis of the cytoskeleton dynamics in the microvilli of intestinal cells. Biophys. J. **88:**1467–1478.
21. **Zhou, X.-H., Y.-Q. Qiu, H.-C. Shi, T. Yu, M. He, and Q. Cai.** 2009. A new approach to quantify spatial distribution of biofilm kinetic parameters by in situ determination of oxygen uptake rate (OUR). Environ. Sci. Technol. **43:**757–763.

Downloaded from http://aem.asm.org/ on February 3, 2015 by guest